Design of a Pulse Sensor to Detect Medium Activity in UWB Networks

Nathaniel J. August, Hyung-Jin Lee, and Dong Sam Ha

Abstract—**Impulse-based ultra wideband (I-UWB) is an attractive radio technology for large ad hoc and sensor networks due to its robustness to multipath effects, sub-centimeter ranging ability, simple hardware, and low radiated power. Current medium access control (MAC) protocols for I-UWB target small wireless personal area networks (WPANs) and cellular networks, but they are not suitable for large, multihop ad hoc and sensor networks. In a previous work, we proposed a method, termed pulse sense, to quickly, reliably, and efficiently detect medium activity in an I-UWB network. Pulse sense enables a distributed MAC protocol for I-UWB radios that is similar to carrier sense multiple access (CSMA) in narrowband systems. This paper investigates CMOS RF circuit implementation of a pulse sensor and its system level design considerations. Simulation results show that the proposed implementation is practical and improves the network performance.**

Index Terms— **Ultra Wideband, Ad Hoc and Sensor Networks, Medium Access Control, Carrier Sense, Pulse Sense, CMOS**

I. Introduction

Compared to narrowband systems, UWB has lower radiated power and a higher data rate, which can be traded for longer range or more robust operation. Due to these and many other advantages, UWB is an attractive radio technology for ad hoc and sensor networks [1],[2]. Such networks enable applications such as inventory tracking, radio frequency identification (RFID), home networking, or structural integrity monitoring. These applications must manage a large number of low-power, low-cost nodes without an infrastructure.

Two forms of UWB signaling have been pursued recently, and they vary in the method used to fill the spectrum. At one extreme, a sharp impulse fills the band as in impulse-based UWB (I-UWB) [3]; and at the other extreme, many simultaneous narrowband tones fill the band as in multi-carrier UWB (MC-UWB), [4]. For ad hoc and sensor networks, I-UWB has several advantages over MC-UWB including robustness to harmful multipath effects, sub-centimeter ranging ability, and low-cost, low-power hardware.

In I-UWB signaling, a sharp pulse (often a Gaussian shape) may occupy several GHz of spectrum, but only lasts hundreds of picoseconds. The low duty cycle pulse repeats at a pulse repetition interval (PRI) of nanoseconds to microseconds.

In wireless networks, the medium access control (MAC) protocol performs the important function of mitigating interference among nodes. Current MAC protocols for I-UWB target small wireless personal area networks (WPANs) and cellular networks [3],[4],[7],[8]. These centralized approaches are a good strategy for small networks with heavy traffic and strict Quality of Service (QoS) requirements. However, in large ad hoc and sensor networks, these protocols impose impractical constraints such as central coordination (which leads to a central point of failure), more complex hardware, or control traffic overhead.

We investigate a simple, distributed MAC protocol that is suitable for I-UWB radios in large ad hoc and sensor networks. In a distributed protocol, each node independently decides to transmit without central synchronization or control. Thus, distributed protocols do not add control traffic overhead, require central coordination, or significantly complicate hardware. Many distributed MAC protocols are based on carrier sense multiple access (CSMA). Carrier sense is also known as clear channel assessment (CCA), and narrowband systems implement CCA by detecting in-band energy. CCA provides two important services: (i) detecting an incoming packet and (ii) checking the channel status before transmitting.

In a previous work, we proposed a method called pulse sense to detect I-UWB medium activity reliably, quickly, and efficiently [9]. We have shown that the method is viable at the system level, and this paper investigates RF implementation of a pulse sensor and its impact on the network performance. With the pulse sensor, an I-UWB network can implement a base MAC protocol similar to CSMA – pulse sense multiple access (PSMA) – that enables distributed medium access.

II. Preliminaries

A. Existing Methods for CCA in I-UWB

The narrow pulses, low radiated power, harsh channel conditions, and strict FCC power limits combine to make CCA difficult for I-UWB systems. As compared to a receiver, a CCA circuit should cost much less and dissipate much less power. Further, a CCA circuit should reliably and quickly detect medium activity. Because I-UWB systems cannot simply detect energy in a certain frequency band, existing CCA circuits for I-UWB traffic do not meet the above goals.

Manuscript received March 31, 2005.

N. J. August, H.-J. Lee, and D.S. Ha are with the Virginia Tech VLSI for Telecommunications (VTVT) Lab, Electrical and Computer and Engineering Department, Virginia Tech, Blacksburg, VA 24061 (phone: 540-231-4942; e-mail: {nateaugu, hlee, ha}@ vt.edu).

A peak detector is a simple method, and it is incapable of separating a wideband I-UWB signal from a strong narrowband signal. This is a problem because I-UWB is meant to coexist with narrowband devices.

A matched filter seems like an ideal method to detect an impulse signal, since it does not require synchronization [5]. However, the complexity of a matched filter makes it more suitable for reception than for CCA purposes. An analog matched filter is not adaptable to dynamic channel conditions and pulse shapes, and it is complex in hardware design. A digital matched filter dissipates significant power, because it requires a fast ADC with wide dynamic range. To adapt to unknown channel conditions, the digital filter also requires a long training period and a large number of taps.

In existing I-UWB systems, correlation is used to acquire an incoming transmission. Correlation may employ a serial or a parallel approach. In terms of hardware complexity, serial correlation provides the simplest circuit for detection, but the long sensing time (possibly in excess of 1000 symbols) makes it unsuitable for CCA purposes [5]. A parallel correlation improves acquisition speed but at the cost of high circuit complexity, so it is also unsuitable for CCA.

An interleaved periodic correlation processing (IPCP) pulse detection system is especially useful for harvesting the combined energy of all multipaths. The IPCP operates by correlating the received signal with samples of itself delayed by one PRI [10]. IPCP is mostly useful for detecting homogenous radar signals in the absence of inter-symbol interference (ISI), co-channel interference, and modulation, which all produce differences between successive symbols. These differences cause the received signal to be less correlated with a delayed version of itself, which degrades the performance. Timing jitter and noise cause further degradation due to the long integration period and sharp correlation peak.

Pulse sense is designed to be robust to the weaknesses of the above systems. It meets the goals of low power dissipation, simple circuitry, reliable detection, and short detection time.

B. *I-UWB Receiver System Architecture*

This section reviews our I-UWB receiver architecture designed for ad hoc and sensor networks. The architecture specifically targets CMOS implementation because of its low power dissipation and low cost. The receiver components have been designed and fabricated in a 0.18 µm CMOS process.

The receiver employs the frequency domain approach in Fig. 1 [6],[11],[12]. A low-noise amplifier (LNA) feeds typical narrowband resonator filters realizing the second order transfer function $1/(s^2+(k\omega_o)^2)$. A filter captures an in-band spectral component of the received signal at frequency f_i, where $f_i = kF_0$ for an integer k. The fundamental frequency F_0 is determined by an observation period T_p such that $F_0=1/T_p$. Next, the ADC captures spectral samples at the pulse repetition rate, which is much lower than the Nyquist over-sampling rate. The reduced sampling rate is suitable for CMOS, and it saves power as well as circuit complexity. The energy harvester harvests multipath energy and performs baseband signal processing operations in the frequency domain, which results in efficient hardware.

The pulse sense block reliably, quickly, and efficiently detects I-UWB medium activity just as carrier sense detects signals in a certain frequency band [9].

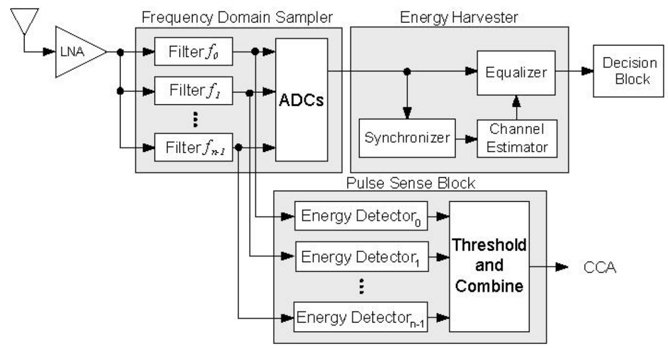

Fig. 1: I-UWB Receiver with Pulse Sense Block

III. Circuit Implementation

For an I-UWB signal, the frequency domain representation spreads the power over a wide spectrum. Therefore, the pulse sense block examines the spectral power components – which are always present – of the signal to avoid the challenges associated with searching for a signal in the time domain.

Our proposed pulse sense implementation shares an LNA, antenna, and filters with the receiver in Fig. 1. The antenna passes signals to a wideband low-noise amplifier (LNA), and the amplified signal is fed to the bank of resonator filters.

We constrain the center frequencies of the filters to multiples of the pulse repetition frequency (PRF), or $1/T_f$, because spectral lines occur at integer multiples of the PRF. This is explained by examining the power spectral density (PSD) of an I-UWB signal with linear modulation, such as BPSK, PAM, or OOK [13]

$$\Phi_{ss}(f) = \frac{\sigma_i^2}{T_f}\left|P(f)\right|^2 + \frac{\mu_i^2}{T_f^2}\sum_{m=-\infty}^{\infty}\left|P\left(\frac{m}{T_f}\right)\right|^2 \delta\left(f-\frac{m}{T_f}\right) \quad (1),$$

where δ is the impulse function, μ_i is the mean of the information sequence, and σ_i^2 is the variance of the information sequence. The second term represents discrete frequency components spaced every $1/T_f$. Thus, the spectrum contains discrete components if $\mu_i \neq 0$. A similar analysis holds for a PPM scheme with $N_s - 1$ pulse positions [14].

$$\Phi_{ss}(f) = \frac{1}{T_f}\left|P(f)\right|^2\left\{1-\left|\Phi_{ii}(fT_p)\right|^2\right\} + \frac{1}{T_f^2}\sum_{m=-\infty}^{\infty}\left|P\left(\frac{m}{T_f}\right)\right|^2\left|\Phi_{ii}\left(\frac{mT_p}{T_f}\right)\right|^2 \delta\left(f-\frac{m}{T_f}\right) \quad (2)$$

where $$\Phi_{ii}(f) = \sum_{k=0}^{N_s-1} p_k e^{j(2\pi fk)} \quad (3)$$

From Section II.B, $f_i = kF_0$, and now also $f_i = n$PRF for an integer n. Thus, the PRF and the center frequency f_i should be harmonically related.

Fig. 2 shows the basic differential LC tank circuit for a resonator filter. Although an infinite quality factor Q is desirable for both the inductor and the capacitor in an LC tank circuit, finite Q is inevitable in an integrated circuit. Because integrated capacitors generally provide a much higher quality factor compared to integrated inductors, our implementation concentrates on the inductor implementation. We measure a Q of up to 14 in TSMC 0.18 μm CMOS technology, and this limits the performance of the LC tank circuit.

The main consideration of the LC tank circuit is the RC time constant, which determines the resonant energy loss over time. A high quality factor in an inductor means a small resistor in series with the inductor, and this can be interpreted as a large parallel resistance in an equivalent parallel RLC model. Therefore, a high Q provides a long RC time constant, resulting in low energy loss. A low Q provides a short RC time constant and attenuates the oscillation energy. In Section V, we explain two designs targeted for short or long RC time constants (relative to the PRI), depending on the achievable Q. The circuit achieves its maximum amplitude quickly and independently of the RC time constant because of the initial energy stored in the shunt inductors.

The small-signal drain to source resistance (r_{ds}) of M1 and M2 also contributes to the equivalent parallel resistance of the LC tank circuit as the parallel combination of the equivalent parallel resistance of the inductor and r_{ds}. Thus, large r_{ds} is desirable to achieve a long RC time constant. To increase r_{ds}, one may decrease the transistor size or decrease the DC bias current. Both approaches decrease the gain, possibly below unity. Therefore, we apply a cascode topology that implements a large series r_{ds} through M1 and M3 (or M2 and M4). The resulting circuit provides high gain and suppresses energy loss.

The inductors labeled L_s prevent leakage through the parasitic gate-to-drain capacitance. They can also compensate for the gate-to-source capacitance for matching purposes.

Fig. 3 shows the impulse response for a train of impulses at a 0.4 GHz PRF, and the circuit resonates at around 6 GHz. Note the fast rise time and exponential decay time.

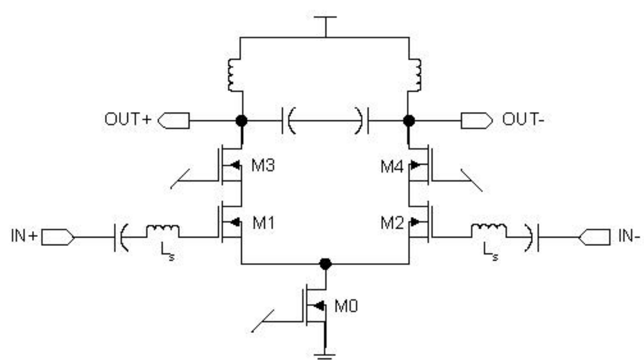

Fig. 2: LC Tank Filter Circuit

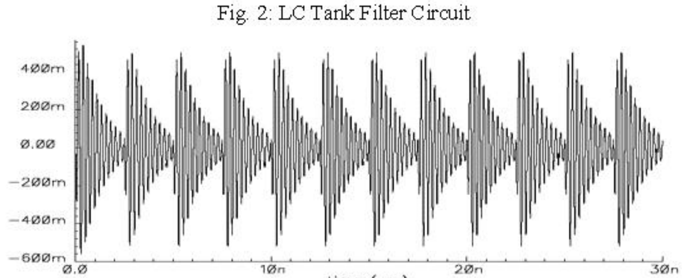

Fig. 3: Impulse Response of Filter Circuit

After the filters capture power spectral components of the received signal, the circuit performs CCA with three additional operations: energy detection, thresholding, and combining.

The energy detectors detect the spectral power components captured in the filter oscillations. The implementation of the energy detector is a simple envelope detector followed by an optional integrator. The integration period should be at least $1/f_0$ to capture the energy of at least one full oscillation in each filter. The maximum $1/f_0$ as mandated by FCC regulations is 0.32 ns (1 / 3.1 GHz), and longer periods of integration harvest more signal energy but also more noise. Further, a longer time period increases power dissipation. Thus, the integration period is a compromise between receiver characteristics and power dissipation. RF CMOS designs of narrowband envelope detectors are well-studied in the literature [15].

Each energy detector reports the presence or absence of a spectral power component at a frequency f_i. These spectral power components are combined with the purpose of detecting the presence of an I-UWB signal while rejecting false alarms from narrowband radios. To this end, the circuit ensures that the majority of spectral components match the low power footprint of an I-UWB signal. We consider two possible methods of combining the spectral power components.

The first option performs threshold detection on the output of each energy detector and combines the outputs of the threshold detectors. This is analogous to a hard decision, so it is termed a *hard combination*. Fig. 4 (a) shows the hard combination scheme. The threshold detectors generate binary values. The circuit reports activity if the sum of binary values exceeds a threshold value X. The hard combination is robust to a strong narrowband interferer, and the sum and comparator blocks may be implemented efficiently with digital circuits.

The second option combines the outputs of the energy detectors and then performs threshold detection on the sum. This is analogous to a soft decision, so it is termed a *soft combination*. Fig. 9 (b) shows the soft combination scheme. The outputs of the energy detectors must pass through limiters so that a strong narrowband interferer does not dictate the final decision. The soft combination gives more accurate weights to the spectral components, but the limiter and the adder circuits are implemented in analog circuitry. The components in either combination scheme are also well studied in RF design.

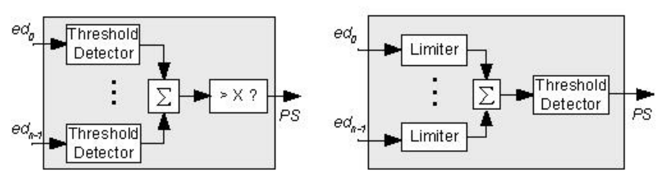

(a) Hard Combination (b) Soft Combination

Fig. 4: Combination and Threshold Blocks

IV. System Design Considerations

A CCA circuit should have a short sensing time (e.g., IEEE 802.15.4 specifies eight symbols) and report a high probability of detection P_d and a low probability of false alarm P_{fa}.

First, the time limit is necessary to prevent the circuit from reporting stale, useless information, as well as to reduce the power dissipation. Fig. 5 shows the throughput for an I-UWB network as CCA time increases. The linear network topology consists of three nodes A-B-C, which are within range of each other, and A and C transmit to B. The time between packets follows a Poisson distribution such that A and C each transmit at an average rate of 0.5×*offered load*, where the offered load is the rate (in bps) that data arrives at the MAC layer from an upper layer over all nodes. Long CCA times degrade throughput, because the information about the state of the medium is outdated and useless.

Due to the narrow pulses, low radiated power, harsh channel conditions, and strict FCC power limits, a reasonable time to acquire an I-UWB signal with a serial correlation is between 800 to 1600 symbols (800 μs and 1600 μs at a 1 Mpps pulse rate [5]). Such CCA times significantly reduce throughput and cause network instability at high offered load. To avoid this performance degradation, we target a sensing time for pulse sense of less than ten symbols, because the performance remains within 1% of the best case CCA time of one symbol.

Next, the pulse sense circuit may decide that a signal is present with a probability distribution of $p_r(x)$ when the signal is actually present with a probability distribution of $p_s(y)$, which is unknown *a priori*. For a joint probability distribution with $x \in$ [**present**, **not present**], the probability $P_{fa} = P(p_r(x = \textbf{present}) \mid p_s(y = \textbf{not present}))$ is called the probability of false alarm. The circuit decides based upon a constant threshold level, so a false alarm occurs due to noise energy only and the false alarm probability P_{fa} is constant. Likewise, the probability of detection P_d is $P(p_r(x = \textbf{present}) \mid p_s(y = \textbf{present}))$.

The number of "looks" refers to the number of times that the circuit performs the combination and threshold operations. Additional looks will increase P_d and decrease P_{fa} at the expense of additional operating time and power dissipation. Assuming each look is independent, the probability of N false alarms (FAs) or detections (Ds) within M looks is

$$P(N\,\mathrm{FAs}) = \binom{M}{N} P_{fa}{}^{N}\left(1 - P_{fa}\right)^{M-N} \qquad P(N\,\mathrm{Ds}) = \binom{M}{N} P_{d}{}^{N}\left(1 - P_{d}\right)^{M-N} \quad (4).$$

The circuit reports a detection if a signal is detected at least N times within M looks.

$$P_{fa}^{cum} = \sum_{i=N}^{M} P(i\,\mathrm{FAs}) \qquad P_{d}^{cum} = \sum_{i=N}^{M} P(i\,\mathrm{Ds}) \qquad (5)$$

For M = 3, 5, or 7 looks, we require that $N = \lceil M/2 \rceil$ for detection. Fig. 6 shows P_{cum} vs. p for probabilities ranging from 0 to 1 for [M=3, N=2], [M=5, N=3], and [M=7, N=4]. The x-axis represents the probability of detection or false alarm that a circuit achieves with one look. The y-axis shows the corresponding cumulative probability from (5) over multiple looks. Thus, the straight line p=p designates the probability for one look. For a useful system, $P_d > 0.5$ and $P_{fa} < 0.5$; otherwise the performance is worse than guessing. In Fig. 6, if $P_d > 0.5$ and $P_{fa} < 0.5$, then the cumulative decision always increases P_d and decreases P_{fa}. Larger M results in better performance, but increases sensing time and power dissipation. A designer may determine specific trade offs among P_d, P_{fa}, sensing time, and power dissipation for a given application.

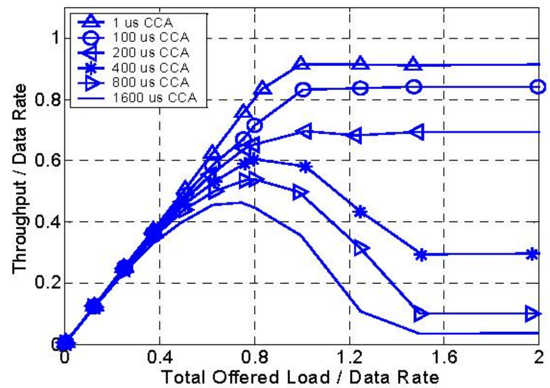

Fig. 5: Throughput for PSMA as CCA Time Increases.

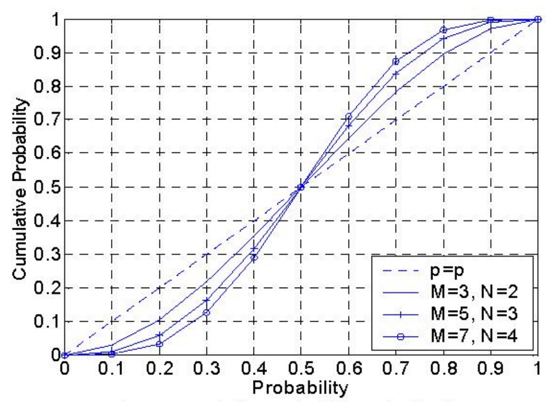

Fig. 6 Cumulative Probability Distribution

V. Simulation Results

The CCA circuit in Fig. 1 was modeled in SPICE and simulated for a 2.5 ns PRI to show our approach for both long and short RC time constants. A longer PRI, PRI_{long}, would improve the link budget by 10 $\log_{10}(PRI_{long}/2.5\text{ ns})$ dB, and the necessary RC time-constants are attainable for PRIs below 1000 ns. We simulate eight filter banks with center frequencies f_0 = 4 GHz, f_1= 4.8 GHz, …, f_9 = 9.2 GHz, and the frequency bandwidth of interest is 3.1~10.6 GHz. Because the inductance determines the center frequency, each filter has the same RC time constant.

We first describe the design of a pulse sense circuit for a short RC time constant, defined as τ < PRI. A short RC time constant may be unavoidable in certain technologies, especially for long PRIs. Fig. 7 shows the simulated response of the filters as an I-UWB pulse train is applied to the inputs. The top graph shows the incoming pulse train, and the bottom graph shows the response of the resonator filter at frequency f_0. For a short time constant, the circuit should capture the pulse train energy for one full PRI, because this guarantees that the unsynchronized circuit captures the peak oscillation energy. One advantage of a short time constant is that successive pulses do not interfere with each other destructively.

Next, we describe the design of a pulse sense circuit with a long RC constant, defined as τ > PRI. Long RC time constants are desirable for energy recovery, although they may be hard to achieve depending on the implementation technology and PRI. Fig. 8 shows the incoming pulse train and the oscillations of filter f_0. For a long RC time constant, a design challenge is that successive pulses with opposite polarity may trigger oscillations out of phase with each other. In the figure, pulse polarity changes between the first and second pulses, between the second and third pulses, and between the fifth and sixth pulses. When the polarity reverses, oscillations from successive symbols combine destructively to reduce the captured energy. This is also predicted from (1), because $\mu_i = 0$ for a long BPSK pulse train.

To prevent destructive combination, we propose solutions, which are only necessary when the achievable τ is greater than the PRI. The first solution is to use a modulation scheme other than BPSK. Candidates include PPM or OOK. For OOK, μ_i in (1) is non-zero. In the time domain, successive OOK pulses (if they exist) have the same polarity. To ensure detection, the preamble should include a string of "on" pulses. For PPM, (2) guarantees the existence of spectral lines. In the time domain, if the time between pulse positions is an integer multiple of $1/f_0$, then a pulse train will create in-phase oscillations regardless of the relative positions of successive pulses.

The second solution is targeted for BPSK modulation. By adding a squaring circuit at the inputs of the resonator filters, successive BPSK pulses will arrive with the same polarity to prevent destructive combination. In (1), this makes μ_i non-zero as seen by the filters. Fig. 9 shows that the oscillation amplitude increases as successive pulses arrive. The oscillations last well into successive PRIs, whereas most energy dies out with a short RC time constant. In the steady state, the oscillations under a long RC time constant are approximately the same amplitude over the entire PRI. This suggests that a circuit can improve performance or reduce power as compared to a short RC time constant.

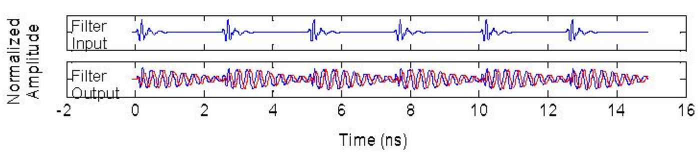

Fig. 7: Filter Response with Short (τ < PRI) RC Time Constant

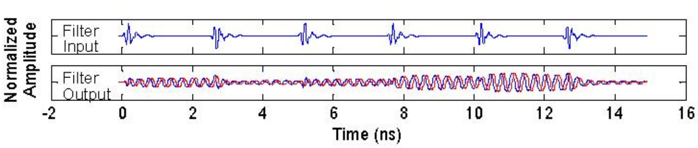

Fig. 8: Filter Response with Long (τ > PRI) RC Time Constant

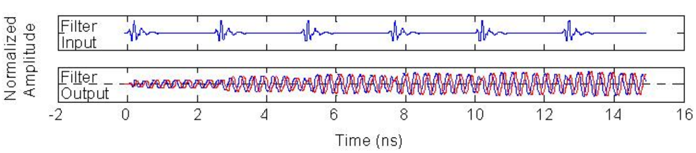

Fig. 9: Filter Response with Long RC Time Constant and Squaring Circuit

Next, we simulated the circuit in Matlab with parameters extracted from the SPICE layout. We start with an Additive White Gaussian Noise (AWGN) channel because performance does not differ significantly with the addition of a channel model [9]. We set the E_b/N_0 at 12 dB, which corresponds to a link distance of 10 m for an 11 dB noise figure at the antenna terminal. At this distance, the receiver can demodulate coded data with a bit error rate (BER) of approximately 2×10^{-4} in the NLOS CM4 channel.

For reference, we derive the theoretical performance of the soft combination scheme in AWGN. When passed through a narrowband filter such as the ones in Fig. 2, the noise assumes a Rayleigh distribution [16]. For a threshold voltage V_T, the probability of a false alarm is

$$p(N > V_T) = \int_{V_T}^{\infty} \frac{R}{\sigma^2} e^{-\frac{R^2}{2\sigma^2}} dR = e^{\left(-\frac{V_T^2}{2\sigma^2}\right)} \quad (6)$$

When the filters resonate with a pulse train input, the probability of detection is [16]

$$p_s(S+N > V_T) = \int_{V_T}^{\infty} \frac{R}{\sigma^2} e^{-\frac{R^2+A_{eff}^2}{2\sigma^2}} I_0\left(\frac{RA_{eff}}{\sigma^2}\right) dR \quad (7)$$

The function I_0 is a modified Bessel function of zero order. Because of the RC time constant of the filters, the effective output amplitude at steady state is denoted A_{eff}.

$$A_{eff} = \frac{\int_0^{T_p} A\left(1-e^{-t/RC}\right) + \int_{T_p}^{PRI} A e^{-t/RC}}{PRI} \quad (8)$$

Fig. 10 compares the performance of the circuit implementation to the above analysis and to our previous system-level simulations in AWGN [9]. The energy detector takes one look at the filter banks and integrates for 1 PRI. The combination scheme is soft combination. Note that Fig. 10 is for comparison purposes only, and we can significantly improve performance with multiple looks [9]. We use a short RC time constant for consistent comparison with the previous simulations. The implementation performs as well as the previous system-level simulations, and both simulations match the expected performance from analysis.

Fig. 10 also shows that the addition of channel model CM1 [17] does not significantly degrade performance [9]. This is because the pulse sense circuit is essentially an energy detector, and the channel model disperses energy but does not cause any loss of energy.

Fig. 11 also shows the performance of the system with an RC time constant twice as long as in Fig. 10 and with a squaring circuit at the filter inputs. The implementation matches expectations, and the performance improves as compared to a shorter RC time constant at the expense of some additional hardware.

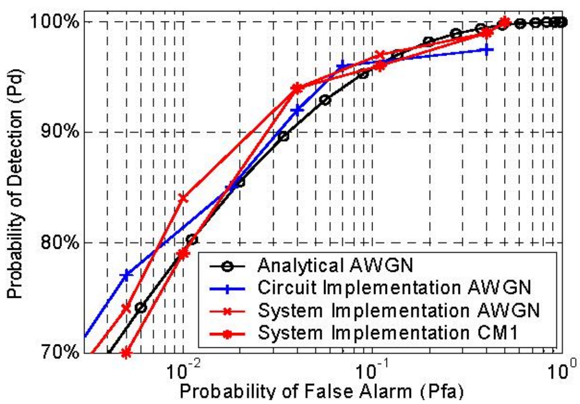

Fig. 10: Comparison of Circuit-Level Implementation, Analytical Expression, and System-Level Implementation for Short Time Constant.

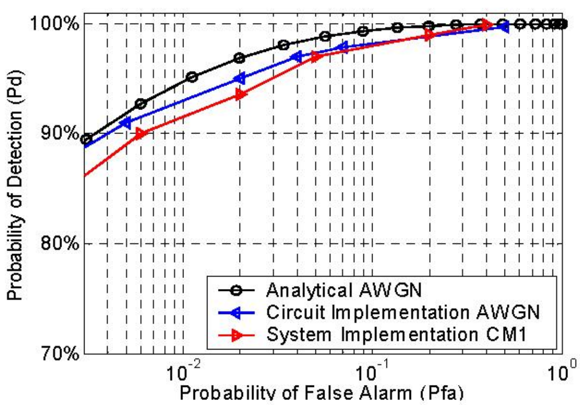

Fig. 11: Comparison of Circuit-Level Implementation, Analytical Expression, and System-Level Implementation for Long Time Constant.

VI. Conclusion

Impulse-based ultra wideband (I-UWB) is an attractive radio technology for large ad hoc and sensor networks due to its robustness to harmful multipath effects, sub-centimeter ranging ability, simple hardware, and low radiated power.

Current MAC protocols for I-UWB are centralized and target small WPANs and cellular networks. The central coordination increases complexity and overhead, and it also leads to a central point of failure. Therefore, large ad hoc and sensor networks usually implement distributed MAC protocols, which generally realize random access and require a method of CCA. The low duty cycle, low power, spectral lines, and harsh channel conditions of I-UWB present difficulties. Existing methods of CCA are either inaccurate or require a prohibitive amount of time or hardware complexity. We propose pulse sense to overcome the challenges of quickly, reliably, and efficiently sensing medium activity in an I-UWB network. The key idea of pulse sense is to examine the spectral power components of the received signal.

Previous results have shown that pulse sense is insensitive to multipath interference, in-band interference, inter-symbol interference (ISI), timing jitter, and narrowband interference. This paper studies the implementation of pulse sense for ad hoc and sensor networks. The proposed implementation is much less complex than a receiver, and it does not require any sampling or synchronization. Because there is no stored template signal, the circuit does not have to dynamically adapt to changing channel conditions and distortions of the pulse shape. It reliably detects I-UWB activity, and it is faster than existing methods by orders of magnitude. Simulations and analysis show that pulse sense is practical for RF implementation in CMOS, and it improves performance at the network level. Thus, pulse sense provides a basic MAC service for I-UWB radios in ad hoc and sensor networks.

References

[1] I.F. Akyildiz, S. Weilian, Y. Sankarasubramaniam, and E. Cayirci, "A survey on sensor networks" *IEEE Communications Magazine*, vol.40, no. 8, pp. 102-114, Aug. 2002.

[2] A. J. Goldsmith and S. B. Wicker, "Design Challenges for Energy-Constrained Ad Hoc Wireless Networks," *IEEE Wireless Communications Magazine*, pp. 8-27, August 2002.

[3] R. Fisher, R. Kohno, H. Ogawa, H. Zhang, M. Mc Laughlin, and M. Welborn, "DS-UWB Physical Layer Submission to 802.15 Task group 3a," doc.: IEEE 802.15-04/137r0, March, 2004. Available: ftp://ftp.802wirelessworld.com/15/04/15-04-0137-00-003a-merger2-proposal-ds-uwb-update.pdf

[4] Anuj Batra, et al., "Multi-band OFDM Physical Layer Proposal for IEEE 802.15 Task group 3a," IEEE 802.15-03/268r3, March 2004. Available: http://www.ieee802.org/15/pub/2003/ Jul03/03268r2P802-15_TG3a-Multi-band-CFP-Document.pdf

[5] V.S. Somayazulu, J.R. Foerster, and S. Roy, "Design challenges for very high data rate UWB systems," Conference Record of the Thirty-Sixth Asilomar Conference on Signals, Systems and Computers, Vol.1, pp. 717- 721, 2002.

[6] H. Lee and D. Ha, "A frequency domain approach for all-digital CMOS ultra wideband receivers," *Proc. 2003 IEEE UWBST Conf.*, pp. 86-90, Nov. 2003.

[7] M.Z. Win and R.A. Scholtz, "Ultra-wide bandwidth time-hopping spread-spectrum impulse radio for wireless multiple-access communications," *IEEE Transactions on Communications*, vol. 48, no. 4, pp. 679-689, Apr. 2000.

[8] The Institute of Electrical and Electronics Engineers, Inc., *802.15.3 Draft Standard Part 15: Wireless Medium Access Control (MAC) and Physical Layer (PHY) Specifications for High Rate Wireless Personal Area Networks*, Draft P802.15.3/D17, Feb. 2003.

[9] N.J August, H.J. Lee, and D.S. Ha, "Pulse sense: a method to detect a busy medium in ultra wideband (UWB) networks," *Digest of Papers Joint UWBST and IWUWBS*, pp. 314-318, May 2004.

[10] I.I. Immoreev, D.V. Fedotov, "Detection of UWB signals reflected from complex targets," *Digest of Papers 2002 IEEE Conference on Ultra Wideband Systems and Technologies*, pp. 193-196, May 2002.

[11] H. J. Lee and D. S. Ha, "A systematic approach to CMOS low noise amplifier design for ultra wideband applications," *Proceedings ISCAS*, to be published May. 2005.

[12] S. Jose, H. J. Lee, and D. S. Ha, "A low power CMOS power amplifier for ultra wideband (UWB) applications," *Proceedings ISCAS*, to be published May 2005.

[13] J. G. Proakis, *Digital Communications*, 4th Edition, McGraw-Hill, New York, NY, 2001.

[14] M. Z. Win, "Spectral density of random time-hopping spread-spectrum UWB signals with uniform timing jitter," *Proc. IEEE Military Communications Conference Proceedings*, vol. 2, pp. 1196 – 1200, Oct. 1999.

[15] T.H. Lee, *The Design of CMOS Radio-Frequency Integrated Circuits*, Second Edition, Cambridge University Press, Cambridge, UK, 2004.

[16] M. L. Skolnik, Introduction to Radar Systems, 2nd Edition, ISBN 0-07-057909-1 McGraw Hill, New York, NY, 1980.

[17] J. Foerster, "Channel Modeling Subcommittee Report (Final)," Technical Report P802.15-02/368r5-SG3a, IEEE 802.15 Working Group for Wireless Personal Area Networks (WPANs), December 2000. http://grouprt.ieee.org/groups/802/15/pub/2002/Nov02/02490r0P802-15_SG3a-Channel-Modeling-Subcommittee-Report-Fianl.zip.